Physica D 40 (1989) 299–310
North-Holland, Amsterdam

A CIRCLE MAP IN A HUMAN HEART

M. COURTEMANCHE[a], L. GLASS[b], J. BÉLAIR[c], D. SCAGLIOTTI[d] and D. GORDON[e]
[a]*Department of Applied Mathematics, University of Arizona, Tucson, AZ 85721, USA*
[b]*Department of Physiology, McGill University, Montreal, Quebec, Canada*
[c]*Centre de Recherches Mathématiques and Département de Mathématiques et de Statistique, Université de Montréal, Montreal, Quebec, Canada*
[d]*The Cardiology Section, Mercy Children's Hospital, Kansas City, Missouri, USA*
[e]*The Division of Cardiology, The Children's Hospital of Philadelphia, Philadelphia, Pennsylvania, USA*

Received 12 April 1989
Revised manuscript received 22 August 1989
Accepted 22 August 1989
Communicated by A.T. Winfree

A circle is divided into two regions, a black one and a white one. Successive iterates of an invertible nonlinear circle map generate a symbolic string indicating whether each iterate is in the black or white region. A number of remarkable properties of the symbolic sequences are described. These properties were previously described for a linear circle map corresponding to a rigid rotation in the "gaps and steps" problem. These results have direct application to a cardiac arrhythmia, parasystole, that results from the competition between two pacemakers in the heart, one in the sinus mode and the other in the ventricles. The theoretical results are directly applicable to a clinical case of a young man who had frequent extra heartbeats.

1. Introduction

Complex rhythms are found in diverse naturally occurring and experimental systems. In recent years there has been intensive interest in developing theoretical tools for understanding the origin of these rhythms, and explaining their basis using mathematical techniques developed for the analysis of nonlinear systems. One particular area of interest has been systems that can be described by nonlinear maps which map the circle into itself f: $S^1 \to S^1$. Circle maps have proved useful in the analysis of dynamics in a large number of physical and biological systems [1].

Our own interest in the properties of circle maps derives from their utility in describing dynamics resulting from the periodic stimulation of cardiac oscillations with brief pulsatile stimuli. Under the assumption that the oscillation is a strongly attracting limit cycle that is rapidly reestablished on a time scale that is short relative to the interstimulus time interval, the effects of periodic stimulation of the oscillation are described by a circle map [2–4]. The circle map can be experimentally measured by delivering single pulses to the oscillation at various phases of the cycle and measuring the resulting phase resetting. The experimentally measured circle map can then be used to compute the effects of periodic stimulation. Extensive experimental studies of an in vitro experimental preparation have shown good agreement with theoretical computations [2–4].

One of the major motivations for studying the properties of periodically stimulated cardiac oscillations in vitro is that they provide a model for some of the abnormal rhythms (arrhythmias) that are known to occur in human hearts. In particular, there are rhythms which arise from the competition between two pacemakers. The normal rhythm is still generated by the normal pacemaker in the

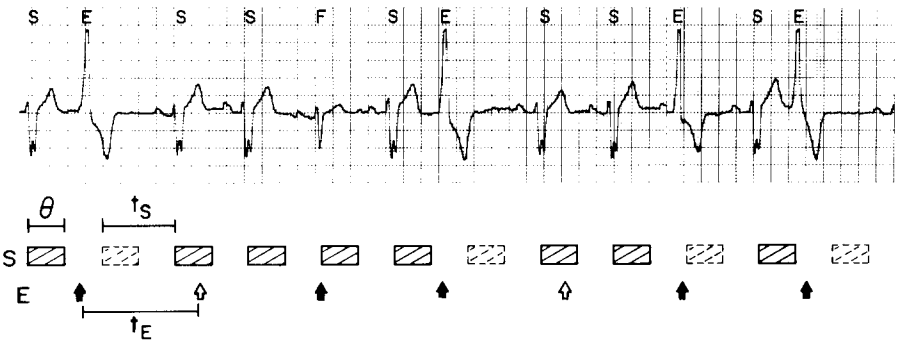

Fig. 1. Electrocardiogram (ECG) from a patient with parasystole. The waveforms are labelled E (ectopic beat), S (sinus beat), F (fusion beat). Below the trace is a schematic representation of the model for parasystole. The left edge of each box represents a sinus pacemaker discharge. The arrows indicate ectopic pacemaker firings. Hatched boxes represent the refractory period (θ); sinus (t_S) and ectopic (t_E) periods are indicated. Filled arrows are ectopic beats falling outside the refractory period. The following sinus beats (dotted boxes) are blocked. Note the correspondence between the simulated rhythm and the ECG. Each box is 200 ms giving $t_E \simeq 1300$ ms and $t_S \simeq 790$ ms.

right atrium, but in addition, there is a second rhythm generated by an abnormal pacemaker located in the ventricles. The normal pacemaker is called the sinus pacemaker and the abnormal pacemaker is called the ectopic pacemaker. The two pacemakers compete for the control of the heart and result in an abnormal rhythm called ventricular parasystole [5]. An example of an electrocardiogram displaying this rhythm is shown in fig. 1. The sinus beats, labelled S, and the ectopic beats, labelled E, are identifiable by their morphology. A schematic interpretation of this rhythm is shown below the trace. The periods of the sinus and ectopic pacemaker are approximately constant and are designated t_S and t_E, respectively. Following each sinus beat is a period, called the refractory time designated θ, during which an ectopic beat is blocked (this means it is not observed). However, if the ectopic beat falls outside of this period it is observed, but the next sinus beat is blocked. The resulting delay is called a compensatory pause. When the sinus and ectopic beats fall at the same time there is a beat of different morphology, called a fusion beat (labelled F).

The situation in which the two pacemakers have absolutely constant frequencies and do not phase reset each other (this is called pure parasystole) has been considered recently [6]. In a more realistic situation, there can be phase resetting of the ectopic pacemaker by the sinus rhythm and the resulting rhythms have been termed modulated parasystole [7–11]. There is a close connection between the mechanism of modulated parasystole and the in vitro experiments of periodically stimulated heart cells; the sinus pacemaker is analogous to the electronic stimulator and the ectopic focus is analogous to the heart cells. This analogy neglects the conduction of excitation through the myocardium, but such factors can be included as a refinement of the basic model [11]. Theoretical tools that are useful in the analysis of the periodically stimulated heart cells are likewise useful in the analysis of rhythms observed in intact human hearts that display parasystolic rhythms.

Our purpose in what follows is to develop theoretical methods to study ventricular parasystole, and to apply the results to analyze this rhythm in a patient. Our consideration of actual clinical data leads to examination of several novel aspects of the dynamics of circle maps.

In section 2 we consider an abstract problem concerning successive iterates of an invertible circle map. The problem is to divide the circle into two regions, labelled 1 and 0, and to describe the symbolic sequences of 1's and 0's generated by iteration. This problem is a generalization of a classical problem in number theory [12]. In section

3 we derive the theoretical model for parasystole (pure and modulated) and show its correspondence to the class of maps discussed in section 2. Section 4 gives a theoretical analysis of ventricular parasystole in a patient. Several of the theoretical predictions about the properties of parasystole can be observed. The purpose of this example is to illustrate to physically minded readers unequivocal evidence that a circle map can be an appropriate theoretical model for clinical data in a patient. Additional clinical examples and a discussion of modulated parasystole from a physiological standpoint is being published elsewhere [11]. A detailed case study of the example in section 4 can be found in ref. [13].

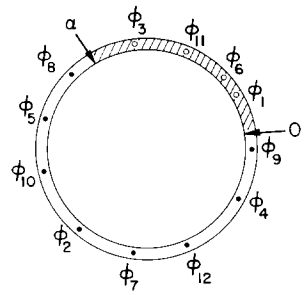

Fig. 2. Iterates of a circle map along a circle. ϕ_1 is the initial phase located in the shaded area between 0 and α (indicated by arrows). We assign the symbol 1 to iterates in the shaded interval and 0 to the other iterates. The sequence of iterates shown here gives rise to the symbolic sequence 101001000010.

2. The gap problem for nonlinear circle maps

2.1. *Definitions*

Consider the continuous map F: $\mathrm{R} \to \mathrm{R}$ with the symmetry $F(t+1) = F(t) + 1$ for all $t \in \mathrm{R}$. By considering $f = F(\mathrm{mod}\,1)$ we restrict the function F to the circle S^1 and thus define a map f: $\mathrm{S}^1 \to \mathrm{S}^1$. f is called a circle map, and from the symmetry condition it is of topological degree 1 [14, 15]. We adopt the notation

$$t_j = F^j(t_0),$$

$$\phi_j = t_j\,(\mathrm{mod}\,1).$$

For most of this paper we assume that f is a monotonically increasing map (an order-preserving homeomorphism). For this case, the rotation number can be defined

$$\rho(f,t) = \lim_{n\to\infty} \frac{F^n(t) - t}{n}.$$

The limit exists and is independent of t. The rotation number is rational if and only if f possesses a periodic orbit [14, p. 102]. If the rotation number is irrational, the dynamics are called quasiperiodic. In this case, provided the function f is of class C^2 the orbit is dense on the unit circle, and the map is topologically conjugate to a rigid rotation with irrational rotation number [14, p. 105]. For convenience, we call such a map a type Q (for quasiperiodic) map.

Consider a circle which is separated into two regions labelled 1 and 0. Start at some initial condition and consider the sequence $\phi_0, \phi_1, \phi_2, \ldots$. Associated with this sequence is the symbolic representation $a_0, a_1, a_2, \ldots$, where a_i is either 1 or 0 depending on the region in which each iterate falls [16]. In fig. 2, the shaded region corresponds to 1 and the white region to 0. Thus, the orbit in fig. 2 corresponds to the symbolic sequence 101001000010. We now start at the first 1 in the sequence and count the number of iterates until the next 1 appears. This process is continued, and used to generate a new sequence of integers called the reduced sequence. For example, the reduced sequence is $2, 3, 5, \ldots$ for the above example.

The reduced sequence contains a number of remarkable properties. These properties have been previously recognized for maps that correspond to rigid rotations in what is known as the gap problem [6, 12], but never to our knowledge for the more general class of monotonically increasing nonlinear C^2 maps of the circle and for order-preserving maps with periodic orbits.

2.2. *The gap problem for type Q maps and order-preserving circle maps with a periodic orbit*

Given a type Q map or an order-preserving map with a periodic orbit the following properties hold for the reduced sequence:

Rule 1. There are at most three integers in the reduced sequence.

Rule 2. Calling these integers m, n and p in increasing order we have $p = m + n$.

Rule 3. At least one of the values of m or n is odd.

Rule 4. One, and only one of the values of m, n or p can succeed itself in the sequence.

These rules hold for both types of maps. However, with type Q maps the usual circumstance is that there are three integers in the reduced sequence, whereas with maps with periodic orbits, there are often either 1 or 2 values in the reduced sequence.

We now demonstrate the rules given above for type Q maps (section 2.2.1) and for maps with periodic orbits (section 2.2.2). In section 2.2.3, we give a method to identify the integer m, n and p for dynamics on a periodic orbit. All three sections are technical, and readers who are interested only in parasystole should skip to section 3.

2.2.1. *Demonstration of the rules for type Q maps*

In order to derive the rules listed above for type Q maps, it is useful to consider the construction shown in fig. 3 [6]. Let α be a number between 0 and 1. The interval $[0, \alpha)$ represents the part of the circle associated with the symbol 1, and the interval $[\alpha, 1)$ represents the part of the circle associated with the symbol 0. Let $f^m(0)$ be the lowest iterate of 0 that lies in $[0, \alpha)$. Since each orbit is dense, we are guaranteed that such an iterate will exist. Let $r = f^{-m}(\alpha)$. Let n be the lowest iterate of α that lies in $[0, \alpha)$. In general, this iterate will fall either in $[0, f^m(0))$ or $[f^m(0), \alpha)$ as shown by figs. 3a and 3b respectively. Assume first that it lies in $[f^m(0), \alpha)$. We show that this leads to a contradiction. Since the interval $[0, r)$ maps to $[f^m(0), \alpha)$, there must be a point b such that $f^m(b) = f^n(\alpha)$. Since the map is one-to-one

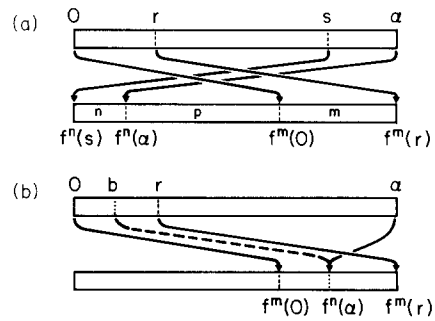

Fig. 3. First return map of the interval $[0, \alpha)$ into itself under the action of a type Q map f. (a) In general, there are three integers, m, n, and p, corresponding to the lowest number of iterates needed to map three contiguous regions in the interval back into $[0, \alpha)$. (b) Illustration of the proof that the lowest iterate of α to return into the interval falls between 0 and $f^m(0)$. If it does not fall in this interval, then we can find an earlier iterate of α, b, which is in the desired interval. See the text.

invertible, $n \neq m$. Suppose $n > m$. Then $b = f^{n-m}(\alpha)$, which cannot be because n is the smallest integer such that $0 \leq f^n(\alpha) < \alpha$. Similarly, we cannot have $m > n$. Therefore, the situation must be as depicted in fig. 3a, where $s = f^{-n}(0)$.

Let p be the smallest integer such that for any u in $[r, s)$, $f^p(u) \in [0, \alpha)$. From fig. 3a, we have

$$0 = f^n(s),$$

$$f^m(0) = f^p(s).$$

Substituting for 0, we find that

$$f^{m+n}(s) = f^p(s).$$

Since f is invertible and has no periodic point, this implies that

$$p = m + n.$$

This argument demonstrates rules 1 and 2. We necessarily have $f(0) \in [\alpha, 1)$, and thus $m > 1$.

To derive rule 3, we show that if both values of m and n are even, some property of the map f is violated. If m and n are even, then p is even since $p = m + n$. Consider a point $t \in [0, \alpha)$. If $f^q(t) \in$

$[0, \alpha)$, $q > 0$, then $q = \sum_{i=1}^{I} c_i$, where $c_i = m$, n, or p. Since m, n, and p are even, then q is even, and $f(t) \in (\alpha, 1)$. Let $v = f(t)$. Then, from above, there are no even iterates, $f^{2j}(v)$, that fall in $[0, \alpha)$. If we let $g(v) = f^2(v)$, then no iterate $g^j(v)$ falls in $[0, \alpha)$. But since f is C^2 with irrational rotation number and $g = f^2$, g is also C^2 with irrational number, and the iterates $g^j(v)$ are dense on the circle. This contradiction proves that at least one of m or n is odd.

Rule 4 can be derived by inspection of fig. 3a. From the construction of the first return map on $[0, \alpha)$, one and only one of the three zones $[0, r), [r, s), [s, \alpha)$ can overlap its image.

2.2.2. *Demonstration of the rules for periodic orbits*

We now show that the four rules stated at the beginning of section 2.2 also hold for a map f when its rotation number is rational, i.e., when a periodic cycle arises. We consider the dynamics on the periodic orbit. This is the asymptotic behavior if the cycle is stable. The argument is based on the construction in fig. 4.

A periodic orbit of length N occurs when, for some $\phi_0 \in [0, 1)$, we have

$$f^N(\phi_0) = \phi_0,$$

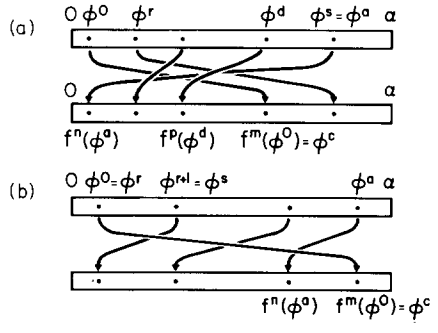

Fig. 4. First return map of the interval $[0, \alpha)$ into itself for the case of periodic orbit. The dots represent the location of the phases of the periodic orbit. This example corresponds to a rational rotation number of 7/11 with 5 iterates in the interval $[0, \alpha)$ in (a) and 4 iterates in the interval $[0, \alpha)$ in (b). In (a) $m = 2$, $n = 1$, $p = 3$ and in (b) $m = 2$, $n = 3$.

and

$$f^k(\phi_0) \neq \phi_0 \quad \text{for } k = 1, 2, \ldots, N-1.$$

In this case, we obtain

$$F^N(\phi_0) = M + \phi_0$$

for some integer M and a rotation number $\rho = M/N$. We assume that $\rho \in [0, 1]$, i.e. $M \leq N$. Let Ω be the set of phases ϕ within the periodic orbit of length N ordered so that their magnitude increases from ϕ^0 to ϕ^{N-1}: $\phi^0 < \phi^1 < \cdots < \phi^{N-1}$. Define the subsets $\Omega_1 = \{\phi^i \in \Omega: \phi^i < \alpha\}$ and $\Omega_0 = \{\phi^i \in \Omega: \phi^i \geq \alpha\}$. The phases in Ω are indicated as small circles on the interval $[0, \alpha)$ in fig. 4.

Since f is order preserving, we can symbolize its action on a phase ϕ^i by a "rotation" through the elements of Ω. We then have

$$f^j(\phi^i) = \phi^{(i+jM) \bmod N}. \tag{1}$$

If either of the subsets Ω_1, Ω_0 contain no iterates of f, the symbolic sequence will contain only 0's and only 1's. We assume that there is at least one iterate in each subset. If there exists only one iterate in Ω_1, then the reduced sequence contains a single number, which is exactly the length of the periodic orbit, N. Figs. 4a and 4b summarize the cases when there are at least two iterates in Ω_1. We use a notation similar to the case of a type Q map.

Let $f^m(\phi^0) = \phi^c$ be the smallest iterate of ϕ^0 such that $f^m(\phi^0) \in \Omega_1$. Such an iterate exists and $\phi^c \neq \phi^0$ since the iterates of f will go through all the elements of Ω before returning to ϕ^0, and there are at least two elements of Ω in Ω^1. Let $\phi^r = f^{-m}(\phi^a)$, where $\phi^a < \alpha < \phi^{a+1}$. Also, let $f^n(\phi^a)$ be the smallest iterate of ϕ^a such that $f^n(\phi^a) \in \Omega_1$. Again this exists and $f^n(\phi^a) \neq \phi^a$. As for the type Q maps, we can show that $f^n(\phi^a) \in \{\phi^0, \ldots, \phi^{c-1}\}$. Let $\phi^s = f^{-n}(\phi^0)$. Now if $\phi^s = \phi^{r+1}$ then only two integers, m and n, are possible in the reduced sequence, fig. 4b. The condition for

having two integers in the reduced sequence is

$$a + nM + 1 = mM \pmod{N}.$$

If the above equality does not hold, there exists at least one integer d between r and s. Let f^p be the lowest iterate of ϕ^d which falls in Ω_1. From fig. 4a, we have

$$\phi^0 = f^n(\phi^s),$$
$$f^m(\phi^0) = f^p(\phi^s).$$

Substituting for ϕ^0, we find that

$$f^{m+n}(\phi^s) = f^p(\phi^s). \tag{2}$$

Since the orbit of any phase $\phi_i \in \Omega_1$ goes through all the phases in Ω_1 before returning to ϕ_i after N iterations, we have

$$N = xm + yn + zp, \tag{3}$$

for some positive integers x, y and z, and

$$N \geq m + n + p,$$

so that eq. (2) implies

$$p = m + n.$$

The above arguments establish rules 1 and 2 for periodic dynamics. The arguments to derive rules 3 and 4 are also similar to those used for the type Q maps, as we now establish.

If there are at least two integers, m and n, in the reduced sequence, one of them will be odd. If not, then all integers in the reduced sequence are even. In this case, N cannot be odd in view of eq. (3). So N is even. Since M and N are relatively prime, M is odd. Consider the iterates $f^{2j+1}(\phi^0)$. Clearly, none of these can be in Ω_1. Since N is even, the odd iterates of ϕ^0 constitute half the elements of Ω_1. If we write $\phi^g = f^{2j+1}(\phi^0)$ then $g = M(2j+1) \bmod N$, and g is odd. So the odd iterates of ϕ^0 will cover all the phases ϕ^g, g odd, in Ω. But $\phi^1 \in \Omega_1$ since there are at least two elements of Ω in Ω_1. This contradiction shows that at least one of m or n is odd.

As in the case of type Q maps, it is clear from fig. 4 that only one of the values in the reduced sequence can succeed itself. Hence we have shown that all four rules apply to the dynamics of f on a periodic orbit.

2.2.3. *Calculation of the reduced sequence for periodic orbits*

We now show how to calculate the possible values of the three integers m, n and p for the periodic orbits described in section 2.2.2, as a function of the rotation number M/N and the number, designated $a+1$, of elements of Ω in Ω_1.

Given the action of f on the elements of Ω as expressed in eq. (1), we wish to find the smallest integers m and n such that

$$jN \leq mM \leq jN + a,$$

for some j, and

$$iN \leq a + nM \leq iN + a,$$

for some i. These are the conditions that must be fulfilled for $f^m(\phi^0) \in \Omega_1$, and $f^n(\phi^a) \in \Omega_1$, respectively. Rearranging each inequation, we find, respectively,

$$0 \leq \frac{M}{N} - \frac{j}{m} \leq \frac{a}{mN} \tag{4a}$$

and

$$-\frac{a}{nN} \leq \frac{M}{N} - \frac{i}{n} \leq 0. \tag{4b}$$

We will illustrate the solution of these inequations for the rotation numbers $\frac{3}{11}$ and $\frac{5}{11}$. It is useful to consider the Farey construction [17] shown in fig. 5. This construction is performed as follows. Starting with $\frac{0}{1}$ and $\frac{1}{1}$, the sums of the numerators and denominators of adjacent fractions are computed, and the resulting fraction, called the mediant, is inserted in the sequence. At the nth step, there are thus $2^n + 1$ fractions (not all of which are shown), and all rational numbers

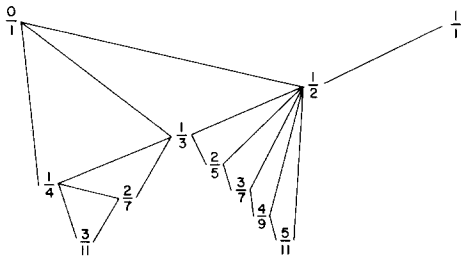

Fig. 5. Farey tree showing the procedure used to obtain the Farey neighbors for a given rational number M/N. Given two ancestors p/q and r/s, the Farey number in the next generation is given by the mediant $(p+r)/(q+s)$. The tree is started using the two ancestors 0/1 and 1/1. Only the ancestors of 3/11 and 5/11 are shown.

eventually appear in the process. The parents of a rational number are the two numbers of which it is the mediant in the Farey construction. The ancestors of a rational number are the reunion of the parents, the parents of the parents, and so forth. For example, the ancestors of $\frac{3}{11}$ are $\frac{0}{1}$, $\frac{1}{4}$, $\frac{2}{7}$, $\frac{1}{3}$, $\frac{1}{2}$ and $\frac{1}{1}$ and the ancestors of $\frac{5}{11}$ are $\frac{0}{1}$, $\frac{1}{3}$, $\frac{2}{5}$, $\frac{3}{7}$, $\frac{4}{9}$, $\frac{1}{2}$, $\frac{1}{1}$.

The following algorithm derives from the observation that the approximation to a rational number provided by its ancestors [17] can be used to solve inequation (4). In our problem M/N is the rational number to be approximated using the ancestors for i/n or j/m. To explicitly obtain the integers m and n, for fixed values of M and N, and a given value of a between 1 and $N-2$, one proceeds as follows:

(a) List all the ancestors of M/N; j/m and i/n in inequation (4) are taken from this set of ancestors;

(b) The minimal value of m is obtained from the ancestor j/m smaller than M/N with minimal denominator within a distance a/mN. The minimal value of n is obtained from the ancestor i/n greater than M/N with a minimal denominator within a distance a/nN.

(c) In case the equality $a + nM + 1 = mM \pmod N$ is not satisfied, there is a third integer, namely $n+m$, in the reduced sequence.

Table 1 gives an application of these rules for the rotation numbers $M/11$, $1 \le M \le 10$.

3. Pure and modulated parasystole

We now draw the parallel between the results above concerning properties of nonlinear circle maps and parasystole. A schematic picture for the dynamics during pure parasystole is shown in fig. 1. The correspondence between the model for pure parasystole and the gap problem (for a rigid rotation of the circle) is described in ref. [6]. We use a notation different from ref. [6] in order to apply the general results of section 2 to the model for modulated parasystole. Consider a circle such as in fig. 2, which represents the ectopic pacemaker

Table 1
The values of m, n and p to return to the interval $[0, \alpha)$ for rotation number $M/11$, where the number of periodic points in $[0, \alpha]$ is equal to $a+1$. Entries with two values correspond to the values m and n, respectively, and entries with three values to m, n and p, respectively.

M	$a=1$	$a=2$	$a=3$	$a=4$	$a=5$	$a=6$	$a=7$	$a=8$	$a=9$
1	10, 1	9, 1	8, 1	7, 1	6, 1	5, 1	4, 1	3, 1	2, 1
2	5, 6	5, 1	4, 1, 5	4, 1	3, 1, 4	3, 1	2, 1, 3	2, 1	1, 2
3	7, 4	3, 4	3, 1	3, 1, 4	2, 1	2, 1	2, 1, 3	1, 1	1, 2
4	8, 3	5, 3	2, 3	2, 1, 3	2, 1, 3	2, 1	1, 1, 2	1, 1, 2	1, 2
5	2, 9	2, 7	2, 5	2, 3	2, 1	1, 1, 2	1, 1, 2	1, 1, 2	1, 2
6	9, 2	7, 2	5, 2	3, 2	1, 2	1, 1, 2	1, 1, 2	1, 1, 2	1, 2
7	3, 8	3, 5	3, 2	1, 2, 3	1, 2, 3	1, 2	1, 1, 2	1, 1, 2	1, 2
8	4, 7	4, 3	1, 3	1, 3, 4	1, 2	1, 2	1, 2, 3	1, 1	1, 2
9	6, 5	1, 5	1, 4, 5	1, 4	1, 3, 4	1, 3	1, 2, 3	1, 2	1, 2
10	1, 10	1, 9	1, 8	1, 7	1, 6	1, 5	1, 4	1, 3	1, 2

cycle. In pure parasystole, successive phases of the normal sinus beats can be obtained by a rigid rotation on that cycle. Let ϕ_i be the phase of a sinus beat in the ectopic cycle. Then the phase of the next sinus beat, ϕ_{i+1}, is given by

$$\phi_{i+1} = \phi_i + \tau \pmod 1,$$

where $\tau = t_S/t_E$.

Depending on the value of its phase within the ectopic cycle, a sinus beat can be placed in different contexts. If $\phi \in [0, \tau - \theta/t_E)$, then the sinus beat is preceded by an ectopic beat. According to our assumptions, the sinus beat is blocked. This is the usual circumstance for ventricular ectopic beats (i.e. there is a compensatory pause [5]). In the event that the next sinus beat is not blocked, the rules derived here have to be modified by adding one sinus beat to the predicted NIB value. If $\phi \in [\tau - \theta/t_E, 1)$, it is preceded by another sinus beat. We wish to consider the possibilities for the number of intervening sinus beats (NIB) between ectopic beats. Clearly, the number of iterates between two successive sinus beats preceded by an ectopic beat gives NIB + 1, since we include a sinus beat which is blocked. Hence, we consider the first return map within the interval $[0, \tau - \theta/t_E)$ which corresponds to the gap problem in section 2.

It is possible to develop a constructive method to determine the zones in the $(\theta/t_S, t_E/t_S)$ parameter space which lead to various values for the number of sinus beats between ectopic beats in the model for pure parasystole [6]. The results of the computations are shown in fig. 6. Each region is labelled by numbers which give the allowed values for the number of sinus beats between ectopic beats. The method used to construct fig. 6 cannot be extended to more general models involving nonlinear circle maps.

We now derive the finite difference equation for modulated parasystole. Call ϕ_i the phase of the ith sinus beat in the ectopic cycle. Assume that the ith sinus beat acts to phase reset the ectopic cycle. Then we expect that the phase of the next sinus beat will be at the phase $g(\phi_i) + \tau$ where $\tau = t_S/t_E$. If $\phi_i \in [0, \tau - \theta/t_E)$, the sinus beat is blocked and will not reset the ectopic pacemaker. In this case, the equation is similar to the equation for pure parasystole. If $\phi_i \in [\tau - \theta/t_E, 1)$, there will be a shift in the phase of the sinus beat given by the function $g(\phi_i)$. Thus, the finite difference equations for modulated parasystole can be written

$$\begin{aligned} \phi_{i+1} &= \phi_i + \tau, & 0 \le \phi_i < \tau - \theta/t_E, \\ \phi_{i+1} &= g(\phi_i) + \tau \pmod 1, & \tau - \theta/t_E \le \phi_i < 1. \end{aligned} \tag{5}$$

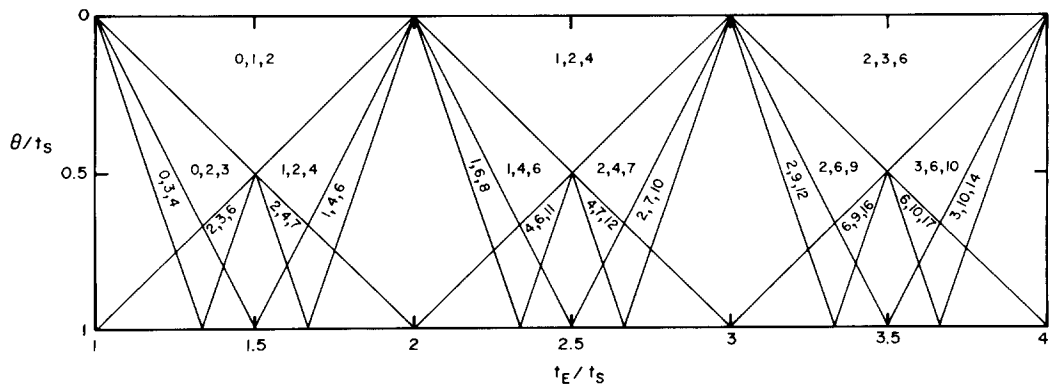

Fig. 6. Allowed numbers of sinus beats between ectopic events, NIB, in the $(\theta/t_S, t_E/t_S)$ plane for pure parasystole. For each region the allowed values are indicated as three integers, separated by commas. To obtain the value for the reduced sequence, 1 should be added to each of the NIB values. Allowed values in the unlabelled regions can be determined from the construction described in ref. [6], which should be consulted for further details on how this diagram is derived. Reproduced from ref. [6].

There are two special circumstances that are of interest. In the limit of no phase resetting, $g(\phi) = \phi$, and the model corresponds to a rigid rotation of the circle. If every sinus beat were effective in phase resetting the ectopic rhythm, the model would be identical to the model for periodically forced nonlinear oscillators in which there is rapid return to the cycle. However, if $g(\phi) = \phi$ for $\phi < \tau - \theta/t_E$, there will be an exact correspondence between the dynamics in this case and the periodically forced case. In fact, the effects of a stimulus early in a cycle in cardiac tissue are often minimal, and therefore, there can be large similarities between the dynamics in both cases. In the event that $g(\phi_i) \neq \phi_i$ for $\phi_i \in [0, \tau)$, there will be discontinuities in the map of eq. (5). This case is not considered here.

As in pure parasystole, the number of iterates required to return into the interval $[0, \tau - \theta/t_E)$ minus one gives the number of sinus beats between successive ectopic beats (NIB); the compensatory pause accounts for the "minus one". The solution of the gap problem, presented in section 2, provides the reduced sequence yielding the required number of iterates. Since the reference cycle is the ectopic rhythm, we directly get the possible NIB values: they are $m - 1$, $n - 1$, and, $m + n - 1 = p - 1$. Depending on the dynamics of eq. (5), we can derive rules based on the properties of the reduced sequence.

If eq. (5) is a type Q map or an order-preserving map with a periodic orbit then the following rules apply to the allowed NIB values:

Rule 1. There are at most three NIB values allowed.

Rule 2. If three NIB values are present, then the sum of the two smaller values is one less than the larger one.

Rule 3. If at least two NIB values are present, one and only one of these is odd.

Rule 4. If three NIB values are present, one and only one of these succeeds itself.

In addition, given the value of the rotation number, $\rho = M/N$, we can determine the possible NIB values and the dependence on the length of the refractory period θ. This is related to the construction described in section 2.2.3 for the gap problem.

Rule 1 is immediate. Rule 2 follows from $(m-1) + (n-1) = m + n - 2 = (m + n - 1) - 1 = (p - 1) - 1$. To obtain rule 3, one must remember from the last section that at least one of m or n is odd, hence at least one of $m - 1$ or $n - 1$ is even. If both are even, then $p - 1$ is odd; if one (hence only one) is odd, then $p - 1$ is even. In either case, rule 3 holds. Rule 4 follows directly from rule 4 about the reduced sequence in section 2.

4. Case report

Section 2 presented abstract results on the symbolic dynamics of circle maps and section 3 applied these results to a mathematical model of a cardiac arrhythmia, parasystole. We now apply these results to analyze dynamics in a clinical record from which fig. 1 is derived. Based on the numerous clinical records we have examined it seems unlikely that the sinus and ectopic pacemakers can coexist without any influence of one upon the other. In this section we assume that there is such an independence of rhythms, i.e. that there is pure parasystole. In this clinical record, the modulation is so weak that we cannot accurately measure the phase resetting function, $g(\phi)$ in eq. (5). Theoretical predictions based on the assumption of constancy of the sinus and ectopic rhythms show close, but not perfect agreement with the data. The point of this example is not to validate the results for modulated parasystole, but to illustrate the quantitatively minded readers that the remarkable subtlety of complex arrhythmias can at least in some cases be partially accounted for by circle maps. Moreover, the theoretical techniques suggested by the mathematical analysis may be readily implemented in computer analysis of arrhythmias. We hope that systematic analyses of long records may be stimulated by this approach. There is an extensive cardiological literature that attempts to decipher the various patterns of ec-

topic activity, but not explicitly in the context of circle maps [8, 18].

We analyze a section of an electrocardiogram (ECG) from a patient with frequent ectopy. The patient had a ventricular abnormality (a ventricular septal defect) corrected at 5 years old and was nonsymptomatic until a sudden fainting spell at the age of 16. A discussion of the possible connections between the parasystolic rhythm considered here, and the arrhythmia that caused the fainting spell (which was probably ventricular tachycardia) as well as additional clinical details and rhythm strips are given in ref. [13]. The record analyzed here was obtained at the start of an exercise test while the patient was standing and was treated with propranolol. Fig. 1 shows an excerpt from the record. Within this short strip, we can identify the common criteria for pure parasystole [5], namely (1) variable coupling intervals from the sinus to the ectopic beats; (2) interectopic intervals which are multiples of a common denominator; and (3) fusion beats. If pure parasystole is indeed the cause of ectopic activity, we should also be able to verify the specific rules derived from the model as well as other theoretical predictions.

The electrocardiographic record was digitized using a Hewlett–Packard (HP) Graphics Tablet hooked up to an HP9816 Computer. All the intervals between successive ventricular activations (ectopic (X) and normal (R)) were digitized to an accuracy of ± 20 ms. Fig. 7a shows a plot of the R–R interval length as a function of time for the record. The values oscillate slightly around an average sinus period of 700 ms. Fig. 7b gives the change in the average ectopic period ($t_{E_{avg}}$) as a function of time, along with the NIB value for each interval. For the cases in which the interectopic intervals contain concealed beats, $t_{E_{avg}}$ is estimated by dividing the X–X interval by the presumed number of concealed beats plus one. The NIB values for each interectopic interval are also indicated on the plot. The values of $t_{E_{avg}}$ obtained are fairly constant around 1300 ms. The only exception is the long interval with NIB = 1

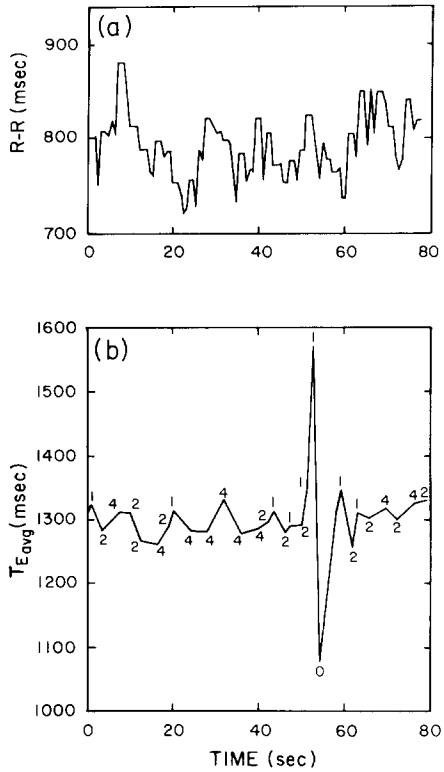

Fig. 7. Clinical data from a patient with parasystole. (a) R–R interval (interval between successive sinus beats) as a function of time for the ECG strip studied. (b) Average ectopic period $T_{E_{avg}}$ as a function of time. When the interval between ectopic beats contains concealed ectopic discharges, the interectopic interval measured on the ECG is divided by the number of concealed discharges + 1. The NIB values for successive interectopic intervals are indicated.

followed by a short X–X with NIB = 0. A similar X–X interval containing a single intervening sinus beat and exceeding 1500 ms in length was observed in an earlier record from this same patient.

Using the values of $t_E = 1300$ ms, $t_S = 790$ ms and $\theta = 430$ ms, we simulate a parasystolic rhythm using the model for pure parasystole. Fig. 8a shows the cumulative histograms of the NIB sequences for both the clinical data and the model. We now consider the transition matrix, which gives the probability of observing a given NIB value (successor) as a function of the preceding value. The rules for parasystole state that when three NIB values are present, one and only one of them can

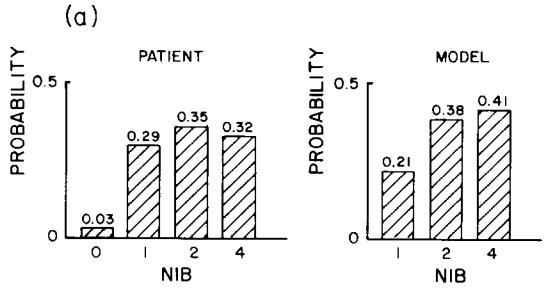

(b)

PATIENT

NIB(i) \ NIB(i+1)	0	1	2	4
0	0.0	0.0	0.0	1.0
1	0.125	0.125	0.625	0.125
2	0.0	0.55	0.09	0.36
4	0.0	0.1	0.5	0.4

MODEL

NIB(i) \ NIB(i+1)	1	2	4
1	0.0	1.0	0.0
2	0.53	0.0	0.47
4	0.0	0.44	0.56

Fig. 8. Comparison between the clinical data and the model for pure parasystole using the parameters (estimated from the data) $t_E = 1300$ ms, $t_S = 790$ ms, and $\theta = 430$ ms. (a) Comparison of the histograms giving the probabilities of observing a given NIB value in the records. The major values are 1, 2, and 4 in both cases. (b) Comparison between the transition matrices for the two cases. The matrices give the probability of observing a given NIB value, NIB($i + 1$), given that the previous value was NIB(i).

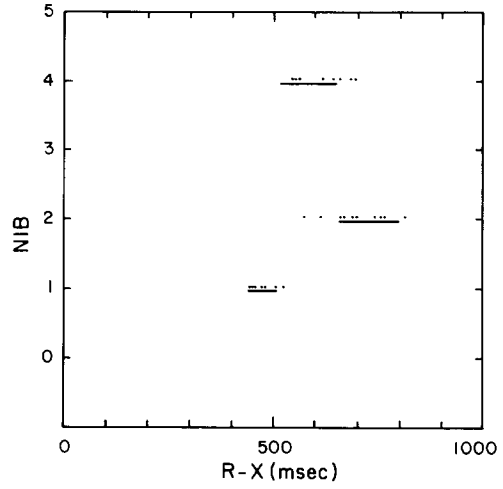

Fig. 9. Relation between NIB values within an interectopic interval and the R–X interval between the last sinus beat and the following ectopic beat in the interval. The dots represent clinical observations, while the solid lines are the intervals observed in the model.

follow itself. The theoretical probabilities for each NIB value in the transition matrix are determined from t_E, t_S and θ. Fig. 8b shows the transition matrices for the ECG strip and the model.

From the construction in fig. 3a, it follows that once the R–X interval from the last sinus beat in an interectopic beat is known, the associated number of sinus beats in the interectopic interval can be determined. Fig. 9 shows this relationship for the theory (solid lines) and the clinical data (dots). The appearance of three distinct regions for the theoretical values is related to the three contiguous regions in the first return map of fig. 3a.

The data in figs. 7–9 show both correspondences and discrepancies with the theoretical model. Most striking are small fluctuations in both the ectopic and sinus cycle times, fig. 7. Thus, the basic assumption of pure parasystole of constant sinus and ectopic cycle lengths and constant refractory time is not satisfied. However, the fluctuations are sufficiently small that many of the major features predicted theoretically are observed experimentally. Thus, the relative frequencies of the NIB values correspond quite closely in the theory and model. The transition probabilities of the NIB values in fig. 8b do not follow rule 4 since all three values 1, 2, and 4 succeed themselves in the clinical data. However, in both the clinical data and the model, 1 is usually followed by 2, 2 is usually followed by either 1 or 4, and 4 is usually followed by 2 or 4. Although the range of R–X intervals associated with each NIB value, fig. 9, are disjoint in the model but not the clinical data, there is a rough clustering of experimental points around the theoretically predicted values. We cannot explain the large (> 1500 ms) interectopic interval in fig. 7b.

We believe that the differences between theory and clinical data in figs. 8 and 9 are most likely associated with the (random?) fluctuations in the t_E, t_S and θ and small interactions between the sinus and ectopic pacemakers. Despite these discrepancies, we believe that the many points of agreement between the theory of parasystole, based on symbolic dynamics of circle maps, and

the clinical data, reveal the power of the theory to give insight into some of the subtle details of the cardiac arrhythmia.

5. Conclusions

The human heart is a complex anatomical structure. The electrical and mechanical events that underly the heartbeat are still poorly understood from a perspective of basic electrophysiology and mechanics. The situation in normal individuals is made increasingly complex in individuals with structural or physiological abnormalities as in the clinical case considered here. Yet, the remarkable finding in this case is that the complex dynamics that are observed clinically can be partially understood based on the dynamics of one-dimensional, invertible circle maps. The particular aspect of the dynamics of circle maps that is considered here, viz. the symbolic sequences giving the itinerary of an orbit on a circle divided into two parts, has been previously considered in mathematics [12, 16]. Yet, the extension of the early results from the "gaps and steps" problem to nonlinear circle maps is original to the best of our knowledge. It is almost magical that the complexities of the intact heart reduce to such a simple mathematical formulation, and a better understanding of the mathematics behind this is still needed. Various aspects of this problem, for example the geometry of the various zones in fig. 6 for the nonlinear maps, are still poorly understood [11].

The application of nonlinear mathematics to study cardiac dynamics reported here is not an isolated observation. Other types of cardiac arrhythmias involving abnormal conduction of cardiac excitation have also been treated using nonlinear mathematics [19, 20]. The theory has predictive value and can serve as a basis for further experimental and clinical studies. The current work weaves an additional thread in the fabric intertwining nonlinear mathematics and cardiac electrophysiology.

Acknowledgements

This research has been partially supported by grants from the Canadian Heart Association and the Natural Sciences and Engineering Research Council (Canada). The clinical study was carried out at the University of Illinois Hospital. We thank the technical and nursing staff for their support and assistance. Thanks to B. Gavin for drawing the figures, S. James for typing the manuscript, and the referees for helpful suggestions.

References

[1] J.A. Glazier and A. Libchaber, IEEE Trans. Circ. Syst. 35 (1988) 790.
[2] M.R. Guevara, L. Glass and A. Shrier, Science 214 (1981) 1350.
[3] L. Glass, M.R. Guevara, A. Shrier and R. Perez, Physica D 7 (1983) 89.
[4] L. Glass, M.R. Guevara, J. Bélair and A. Shrier, Phys. Rev. A 29 (1984) 1348.
[5] L. Schamroth, The Disorders of the Cardiac Rhythm (Blackwell, Oxford, 1980).
[6] L. Glass, A.L. Goldberger and J. Bélair, Am. J. Physiol. 251 (Heart Circ. Physiol. 20) (1986) H841.
[7] G.K. Moe, J. Jalife, W.J. Mueller and B. Moe, Circulation 56 (1977) 968.
[8] J. Jalife, C. Antzelevich and G.K. Moe, Pace 5 (1982) 911.
[9] N. Ikeda, S. Yoshizawa and T. Sato, J. Theor. Biol. 103 (1983) 439.
[10] L. Glass, A.L. Goldberger, M. Courtemanche and A. Shrier, Proc. R. Soc. London Ser. A 413 (1987) 9.
[11] M. Courtemanche, L. Glass, M.D. Rosengarten and A.L. Goldberger, Am. J. Physiol. 257 (Heart Circ. Physiol. 26) (1989) H693.
[12] N.B. Slater, Proc. Camb. Phil. Soc. 63 (1967) 1115.
[13] D. Gordon, D. Scagliotti, M. Courtemanche and L. Glass, Pace, in press.
[14] V.I. Arnol'd, Geometrical Methods in the Theory of Ordinary Differential Equations (Springer, Berlin, 1983).
[15] J. Bélair and L. Glass, Physica D 16 (1985) 143.
[16] G.A. Hedlund, Am. J. Math. 66 (1944) 605.
[17] I. Richards, Math. Mag. 54 (1981) 163.
[18] N.Z. Kerin, M. Rubenfire, R. Stoler and M.N. Levy, Am. J. Cardiol. 57 (1986) 392, and references therein.
[19] A.T. Winfree, When Time Breaks Down: The Three Dimensional Dynamics of Electrochemical Waves and Cardiac Arrhythmias (Princeton Univ. Press, Princeton, 1987).
[20] L. Glass and M.C. Mackey, From Clocks to Chaos: The Rhythms of Life (Princeton Univ. Press, Princeton, 1988).